



**HAL**  
open science

## Quantitative videomicroscopic analysis of the sociologic behavior of non-invasive and invasive tumor cell lines

Jean-Marie Zahm, Salma Hazgui, Manuela Matos, Aadil Ben Seddik, Béatrice Nawrocki Raby, Myriam C. Polette, Philippe L. Birembaut, Noël Bonnet

### ► To cite this version:

Jean-Marie Zahm, Salma Hazgui, Manuela Matos, Aadil Ben Seddik, Béatrice Nawrocki Raby, et al.. Quantitative videomicroscopic analysis of the sociologic behavior of non-invasive and invasive tumor cell lines: Sociologic behavior of cell lines. Cellular and Molecular Biology, 2007, 52 (6), pp.54-60. inserm-00149660

**HAL Id: inserm-00149660**

**<https://inserm.hal.science/inserm-00149660>**

Submitted on 15 Jun 2007

**HAL** is a multi-disciplinary open access archive for the deposit and dissemination of scientific research documents, whether they are published or not. The documents may come from teaching and research institutions in France or abroad, or from public or private research centers.

L'archive ouverte pluridisciplinaire **HAL**, est destinée au dépôt et à la diffusion de documents scientifiques de niveau recherche, publiés ou non, émanant des établissements d'enseignement et de recherche français ou étrangers, des laboratoires publics ou privés.

# **Quantitative videomicroscopic analysis of the sociologic behavior of non-invasive and invasive tumor cell lines**

**Zahm JM<sup>✉</sup>, Hazgui S, Matos M, Ben Seddik A, Nawrocky Raby B,  
Polette M, Birembaut P, Bonnet N**

**INSERM U514, Université de Reims, IFR53  
45 rue Cognacq-Jay 51092 Reims cedex, France  
Fax: (33) 326 06 58 61  
Email: [jm.zahm@univ-reims.fr](mailto:jm.zahm@univ-reims.fr)**

## **ABSTRACT**

To analyze the spatial distribution of tumor cell lines with different invasive properties, we used time-lapse videomicroscopic recordings associated with software programs we have developed for quantification. We observed that non-invasive tumor cells rapidly formed small clusters which aggregated to form larger clusters, whereas highly invasive tumor cells remained isolated and did not form clusters. An attraction index computed from a cellular automaton model was used to quantify the degree of attraction-repulsion between cells. The results suggest that the cluster formation by non-invasive cells is not related to a global attraction model and that the random (dispersed) distribution of invasive cells is not related to cell repulsion. According to these results, we can conclude that random cell movement combined with the intrinsic properties of cells explains the phenomenon of cluster formation.

**Key words:** cluster formation, videomicroscopy, cellular automaton, migration,

**Running title:** Sociologic behavior of cell lines

## INTRODUCTION

Tumor progression is a multistep process during which cancer cells leave the primary tumor, invade the surrounding stroma and disseminate in secondary organs. Accumulating evidence now supports the concept that the acquisition of invasive properties by epithelial cells is associated with the loss of epithelial characteristics and the acquisition of mesenchymal properties, a phenomenon referred as epithelial-to-mesenchymal transition (7, 18). Understanding the mechanisms by which this epithelial-to-mesenchymal transition could occur constitutes one of the tracks that can be followed to find new targets for fighting cancer.

Among the wide type of studies that can be performed in order to characterize invasive/non invasive cell phenotypes, we are interested in studying the collective behavior of cell populations observed under culture conditions. After the pioneering work of Abercrombie (1) in the fifties, it is now recognized that observing the “social” behavior of live cell populations may be as successful as the study of animal (and human) social interaction. The terminology “cellular sociology” is associated to this type of activity (5, 6, 12). Cellular sociology represents a large number of concepts that can be studied at the population level instead of the single cell level: migration, adhesion, cell-cell interaction and communication, cell-extracellular matrix interaction, spatial distribution, etc. Up to now, only a few of these concepts have been studied by using the cellular sociology approach. The mostly studied concept is that of spatial distribution. It has been shown that the arrangement of cells in space is rarely random and that the type of distribution can be put into correspondence with the physiological and phenotypical state of the cell population. Numerous applications have been found in the field of diagnostic or prognostic [2, 17, 21, 23].

Our previous work on the subject (15) shows that, starting from a random distribution, tumor cells in culture behave differently according to their invasive or non invasive properties. Invasive cells remain randomly dispersed until confluence while non invasive cells show a strong tendency to form stable clusters that grow as a function of time. We also showed that the transfection of human E-cadherin cDNA in invasive bronchial tumor cells induced the formation of cell clusters, in relation with a decrease of the invasive abilities of the transfected cells (16). As a first attempt to interpret this

different behavior, we studied the respective role of cell migration and proliferation for invasive and non invasive cell lines. We determined that the parameters quantifying these activities were not significantly different in two dimensional (2D) cultures. [13]. However, more recent work done in three-dimensional (3D) cultures showed that 3D migration is significantly different for a non-invasive cell population and an invasive cell population [9]. If we want to go further in the study of the sociologic behavior of these cell lines, we must be able to answer the question: “why do non invasive cell lines form clusters and why invasive cell lines do not?” Even if we do not go at the molecular level with this type of approach, we must at least be able to identify the gross mechanism that governs this different behavior. One hypothetical mechanism would be that, in the case of non invasive cells, each cell attracts the other ones. In this case, a tiny difference in the spatial density of cells after seeding would be amplified as a function of time: cells in a region of space with a slightly lower density would be attracted by cells in regions of space with a larger density, until cells are sufficiently close together to form small clusters. Then, small clusters continue to attract each other and form larger clusters, until confluence. In the case of invasive cells, this mechanism could be replaced by either the absence of attraction or by an effect of repulsion. In both cases, the spatial distribution of the cells would remain random as a function of time. The other possible mechanism is that there is neither an attraction nor a repulsion effect. In this situation, one can imagine that cells migrate at random, according to a Brownian model. Thus, two cells may come close to each other in a random fashion. When this happens, two possibilities may occur: either the two cells “decide” to form a mini-cluster (due to some molecules present at both cell surfaces, for instance; or a molecule and a receptor) or they “decide” to ignore themselves and continue their random migration until they find an appropriate partner.

The observation of many movies of live cell populations let us think that the first hypothesis (global attraction by non invasive cells) could be the right one. Thus, the aim of the work presented here was to find experimental ways to check the hypothesis on an objective (quantitative) basis. Basically, the idea is to check whether non invasive cells moved in the direction of the largest density of cells (hypothesis of global attraction) or not, and to check whether invasive cells moved in the

direction of the lowest density of cells (hypothesis of global repulsion) or moved independently of the density of cells (hypothesis of absence of global attraction or repulsion).

In an independent work, we verified that the concept of an attraction or repulsion potential could indeed explain the formation of clusters. (3) This was done through simulations made in the framework of cellular automata. The main difference between our cellular automaton and classical ones is that the formal rules that govern our cellular automaton are not localized (i.e. based on the local environment of each cell) but based on the whole set of objects. In this paper, the ideas that were at the origin of the cellular automaton are also used to characterize quantitatively the direction of migration of the individual cells. Using videomicroscopy techniques and appropriate software programs that we developed, the different methods mentioned above, i.e. characterization of the spatial distribution of cell populations as a function of time and test of an hypothesis for the mechanism that governs the formation of clusters by invasive cells were applied to five different cell populations: two invasive ones, two non invasive ones and one intermediate, weakly invasive. To validate the relevance of the parameters computed from the cellular automaton model, we also analyzed the behavior of cells in an *in vitro* model of wound repair, in which cell migration was characterized as a directed migration [24].

## **MATERIALS AND METHODS**

### **Cell lines**

The human bronchial cell lines, 16HBE14o- [10] and BZR [12], were derived from normal human bronchial cells immortalized after transfection with the SV40 large T-antigen gene. The BZR cell line was also infected with the v-Ha-*ras* oncogene. The human mammary epithelial cell lines MCF-7, BT549 and MCF10 were obtained from American Type Culture Collection. Cells were cultured in a 5% CO<sub>2</sub> fully humidified atmosphere at 37°C in Dulbecco modified Eagle's medium (DMEM) (Gibco BRL, Grand Island, USA) supplemented with penicillin, streptomycin and 10% fetal calf serum (Gibco BRL).

### **Model of cell dispersion**

A density of  $2.10^5$  cells per mL was plated into each culture dish (diameter 3.5 cm). One hour after seeding, the culture dish was placed on the stage of a Zeiss IM35 inverted microscope (Zeiss, Oberkochen, Germany) and enclosed in a small transparent culture chamber (Climabox, Zeiss) with 5% CO<sub>2</sub> in air at 37°C. Image sequences were recorded at 10x magnification in the phase-contrast mode with a sampling rate of 1 image per minute for up to 17 hours. Using each image as an individual frame, a movie was constructed so as to obtain a qualitative impression of the cell behavior. One image was subsequently analyzed every 100 minutes.

### **Model of directed migration**

16HBE14o- cells were plated into culture dishes at  $10^6$  cells/ml (diameter 35mm). When the cells had reached confluency, the culture medium was removed from the culture dish. A 1µl droplet of NaOH 1N was deposited in the center of the culture dish and immediately diluted in 1 ml of culture medium. The NaOH droplet created a wound by cell desquamation (24). The culture medium was again removed and the wounded culture was rinsed with 2 ml of culture medium and incubated in 5% CO<sub>2</sub> in air at 37°C. The culture dish was then placed on the stage of the Zeiss IM35 inverted microscope (Zeiss, Oberkochen, Germany) and enclosed in the small transparent culture chamber (Climabox, Zeiss) with 5% CO<sub>2</sub> in air at 37°C. Image sequences of the edge of the lesion were recorded at 10x magnification in the phase-contrast mode with a sampling rate of 12 images per hour until closure of the lesion. Again, using the images as individual frames, a movie was constructed in order to get a qualitative impression of the cell behavior. One image was subsequently analyzed every 30 minutes.

### **Cell cohesion quantitation**

The spatial distribution of cells was characterized and quantified using a cellular sociology algorithmic software based on the use of geometrical models, as described by Nawrocki Raby et al. [15], namely Voronoï's partition and Delaunay's graph [2, 12]. These methods, applied to the set of points locating the position of the cells, provide useful information about the spatial distribution and neighborhood relationships of cells. From each of these methods, several quantitative parameters can be deduced:

- for the Voronoï diagram: average and standard deviation of the areas, area disorder (AD), roudness factor homogeneity (RFH).
- for the Delaunay triangulation: mean (M) and standard deviation (SD) of segment length, length disorder.

### **Quantification of the attraction-repulsion potential of cells**

A software developed in our laboratory was used to quantify the attraction-repulsion potential of cells. An attraction-repulsion index was computed from the recorded image sequences by using a new method for quantifying the degree of attraction-repulsion between cells. This method consisted of computation of the local density of cells in a given experimental image at time  $t$ , according to the kernel-based Parzen method [18]. The kernel size was set to 1/8th of the image size, but the final results are not very sensitive to this parameter. Then, from the next image at time  $t+\Delta t$ , we checked whether individual cells moved in the direction of high cell density, in the direction of low cell density or in a direction not related to density. A rank  $r$  was attributed to each cell ( $0 \leq r \leq 7$ ), corresponding to the direction followed by the cell during its move from image  $t$  to image  $t+\Delta t$  (figure 1). Rank 0 corresponded to a migration towards the lowest cell density and rank 7 to a migration towards the highest cell density. The rank  $r$  was defined cell by cell and since the densities were represented by real values (not integers), the probability that 2 density values were equal was almost null. Non-moving cells were excluded and the threshold used to decide if a cell is moving or not was set to 1 pixel. The index was calculated by averaging and normalizing this rank:

$$index = \frac{1}{3.5N} \left( \sum_{n=1}^N r_n \right) - 1 \quad \text{where } N \text{ and } r \text{ corresponded to the number of cells in the images and}$$

the rank of the cells, respectively.

The index calculated from these considerations is close to +1 for a global attraction model, close to -1 for a global repulsion model, and close to 0 for a model of no global attraction/repulsion.

## RESULTS

### Videomicroscopic analysis of cell behavior

Videomicroscopic and image analysis techniques were used to analyze alterations in the collective behavior of the five cell lines during the time of culture. Phase-contrast images were recorded throughout the time of culture for both the cell dispersion and the directed migration models. Figure 2 represents images of the five cell lines recorded 1, 9 and 17 hours after seeding: from top to bottom, cell lines with a decreasing invasive capacity are displayed. One can verify that the spatio-temporal behavior of these cell lines is very different. One hour after seeding, the 16HBE14o- cells are randomly distributed. After 9 hours of culture, these cells begin to form small aggregates, which become larger clusters after 17 hours of culture. On the contrary, BZR cells are randomly distributed, remain isolated and do not form clusters at any point throughout the time of culture. Other cell lines exhibit an intermediate behavior. It is noteworthy that static images of cells cannot give a good idea of the dynamic cell behavior: from figures 3b and c, one could get the impression that clusters are also produced. This is not the case since pseudoclusters are not stable and are disorganized as soon as they are produced.

The spatio-temporal behavior of 16HBE14o- cells in the directed migration model, which illustrates a model of global attraction, is represented in figure 3. Image of cells located at the edge of the wound were analyzed every 5 min until closure of the wound. We clearly observed the progressive closure of the wound, which was complete within 3 hours.

Analysis of Voronoi's partition and Delaunay's graph from the recorded images indicated that important differences existed for each cell line in relation to interactions between cells. After 2 hours of culture, the 16HBE14o- and BZR cells displayed the same pattern for the graphs of Voronoi and Delaunay (data not shown), but significant differences between the 2 cell lines were observed after 17 hours of culture. Figure 4 displays the spatial localization of cells at 17h of culture and show that the 16HBE14o- cells formed small aggregates, whereas the BZR cells remained randomly distributed. The parameters that we computed to characterize the spatial distribution on a quantitative basis reflected these observed differences and are represented in figure 4 for a non-invasive cell line and an invasive cell line. During the first hours of culture, the 2 cell lines displayed a random distribution. However at

17h of culture the non-invasive 16HBE cell line acquired a cluster distribution characterized by an increase of AD and decrease of RFH for Voronoi's partition and a decrease of M and increase of SD for Delaunay's graph. At the opposite, the parameters calculated from the invasive BZR cell line were not significantly modified during the time of culture.

### **Analysis of attraction or repulsion potential**

The precise issue we wanted to address in the present work is whether or not the behavior of non-invasive and invasive cells could be mediated by a form of global attractive or repulsive potential. From the time-lapse video images, we used an original method for quantifying the degree of attraction-repulsion of cells which allowed us to determine a new parameter: the index of density-based attraction/repulsion, which is close to +1 for a global attraction model, close to -1 for a global repulsion model, and close to 0 for a model of no global-attraction/repulsion. Figures 5A and 5B display 2 successive images of the experimental series recorded at 100 min interval with the non-invasive 16HBE14o- cells. The estimated density of cells is represented in figure 5C where a high cell density, represented by the white-colored area, clearly appeared at the right hand upper corner. The directions of migration of the cells, determined from the successive positions of cell images 5A and B, are superimposed on the estimated density. We can easily observe that the cells do not move systematically in the direction of highest density or outwards the highest density area. The same data obtained with the invasive BZR cell line are reported in figure 5 D, E, F. Here again we observed no particular orientation of the direction of migration of the BZR cell line. The quantitative results reported in figure 6 demonstrate clearly that throughout the time of culture, the non-invasive 16HBE14o- and MCF-7 cells as well as the invasive BT-549, MCF-10 and BZR cells had index values close to 0. This reflects the fact that a model of no global-attraction/repulsion governs their migration. In contrast, we computed from the directed migration model (in vitro wound repair model) an index value close to +1, which corresponds to a model of global attraction (assuming that the center of the lesion represented a density-based attraction).

## DISCUSSION

In this study, we describe techniques using videomicroscopy in combination with cell sociology techniques and a cellular automaton model to analyze the spatio-temporal behavior of non invasive and invasive cell lines. Our methods present the advantage of allowing the dynamic study of the behavior of living cells and clearly demonstrate that the spatio-temporal distribution of the cell lines was quite different. On the one hand, non-invasive cells, which have been previously characterized as expressing membranous E-cadherin and  $\beta$ -catenin, rapidly formed clusters and were very cohesive. In contrast, invasive cells had a random spatial distribution that could be attributed to an absence of E-cadherin and to a cytoplasmic localization of  $\beta$ -catenin [14]. In a previous study, we demonstrated that neither cell migration nor cell proliferation played a discriminatory role in explaining differences in the spatial organization of cell lines characterized by different invasive properties [13]. From these observations, one question remained to be elucidated: could the cell cluster formation exhibited by non-invasive cells be related to a global attraction model, based on the idea of a universal attraction of cells by each other, while that of the random distribution of invasive cells, which did not form clusters, be related either to a loss of this global attraction capacity or to cell repulsion?

To answer these questions, in the present work we investigated under specific culture conditions the migratory behavior of non-invasive cells in which cluster formation does occur, and likewise that of invasive cells that do not form clusters. Furthermore, in order to demonstrate the relevance of the experimental parameters that we calculated, we investigated the behavior of cells involved in a directed migration model represented by an *in vitro* model of epithelial wound. From the image sequences, an attraction-repulsion index was computed so as to characterize whether or not the migratory behavior might be considered random or directed. From the cell dispersion model, we concluded that the behavior of both non-invasive cells and invasive cells was not governed by an attraction/repulsion potential: cell cluster formation by non-invasive cells is not in favor of a global attraction model based on the idea of a universal attraction between cells, while the random spatial distribution of invasive cells is not related to cell repulsion. Therefore, these results emphasize the hypothesis that the random motion of cells combined with cell to cell adhesion capacity (brought about by intercellular adhesion molecules such as E-cadherin) alone could explain the phenomenon of

cluster formation observed in non invasive cells: cells move randomly and have the capacity to adhere to each other. Progressively larger and larger clusters are created, due to both cell proliferation and aggregation of small clusters to each other, for which there is no need to look for a stimulus driving the cells to form clusters or clusters to aggregate themselves. Typically, the motion of the cells in the *in vitro* models of cell dispersion described in the present work can be characterized as a non-directed motion. These results are in agreement with those described by Rieu et al [20] who reported that Hydra cell motion consists of random and correlated parts: random fluctuations of single endodermal cells create clusters by accretion and coherent motion of cells only occurred during rounding of large clusters.

In contrast, we observed that the motion of cells involved in the process of wound repair was directed. This model of directed migration was only used to validate the relevance of the parameters computed from the cellular automaton model. An interesting point to take into consideration for explaining the differential behavior of the 16HBE14o<sup>-</sup> cell line in the dispersion and in the directed migration models would be to study the parameters potentially involved in the control of the direction of cell migration. An “automatic controller of direction” has been described by Gruler [8]. This controller might be able to detect the deviation angle between the direction of migration of cells and the position of the stimulus (either chemical or electrical stimulus) and could induce modifications of the cell trajectories in order to allow the cell to migrate towards the stimulus. We could therefore hypothesize that in the cell dispersion model no particular stimulus is present for directing the cell migration, whereas in the directed migration model the guidance of motility could be related to either chemotaxis or haptotaxis (otherwise known as contact guidance). We have previously shown that large variations of the electric field in wounded cultures occurred during the repair process [25]. We also demonstrated a hyperpolarisation of the membrane potential of migratory cells as compared with stationary cells located far from the wound. In addition, we observed that isolated respiratory epithelial cells, placed in an electric field, acquired a uniform and constant direction of migration in contrast to the random migration of cells not subjected to an electric field. These results suggested that an endogenous electric field could be one of the mechanisms triggering and directing cell migration during wound repair. However, the presence of a mechanically directed movement can not be excluded. A constrain due to

confluency may exist against the free space formed by the wounded area and a resulting binary mechanical gradient could also lead to directed cell migration. It has been previously demonstrated that cells are able to align in response to a uniaxial strain, with a protrusive activity increased at the ends and decreased along the sides of the cells. [11]

In conclusion, the present results confirm the organizational behavior of the cell lines examined here: non-invasive cells formed clusters with a cohesive organization, whereas invasive cells organized in a non-cohesive manner. Videomicroscopic techniques combined with a new density-based cellular automaton model for analyzing whether or not cells attract or repel one another demonstrated that the cell cluster formation was not driven by some form of attraction potential, and that the dispersed distribution of invasive cells was not related to cell repulsion. Random cell movement combined with the intrinsic properties of cell lines constitutes probably a better explanation of the phenomenon of cluster formation.

#### **ACKNOWLEDGMENTS**

We thank Dr. D. Gruenert for providing 16HBE14o- cells and Dr. C.C. Harris for providing BZR cells. Supported by Région Champagne-Ardenne and by a grant in the framework of the “Programme commun INSERM/CNRS Bioinformatique” (2004-2005). S. Hazgui was supported by Association pour la Recherche sur le Cancer (ARC) and Société de Pneumologie de Langue Française (SPLF).

## REFERENCES

1. Abercrombie, M. and Heaysman, J.E.M., Observations of the social behaviour of cells in tissue culture. Speed of movement of chick heart fibroblasts in relation to their mutual contact. *Exp. Cell Res.* 1952, 6: 111-131.
2. Bigras, G., Marcelpoil, R., Brambilla, E. and Brugal, G., Cellular sociology applied to neuroendocrine tumors of the lung: quantitative model of neoplastic architecture. *Cytometry* 1996, 24: 74-82.
3. Bonnet, N., Matos, M., Polette, M., Zahm, J.M., Nawrocki-Raby, B. and Birembaut, P., A density-based cellular automaton model for studying the clustering of noninvasive cells. *IEEE Trans. Biomed. Eng.* 2004, 51 (7):1274-1276.
4. Conzens, A.L., Yezzi, M.J., Kunzelmann, K., Ohrui, T., Eng, K., Finkbeine, W.E., Widdicombe, J.H., and Gruenert, D.C., CFTR expression and chloride secretion in polarized immortal human bronchial epithelial cells. *Am. J. Respir. Cell. Mol. Biol.* 1994, 10:38-47.
5. Dussert, C., Rasigni, M., Palmari, J., Rasigni, G., Llebaria, A. and Marty, F., Minimal spanning tree analysis of biological structures. *J. Theor. Biol.* 1987, 125:317-323.
6. Dussert, C., Kopp, F., Gandilhon, P., Schneider-Pourreau, N., Rasigni, M., Palmari, J., Rasigni, G., Martin, P.M., and Llebaria, A., Toward a new approach in tumor cell heterogeneity studies using the concept of order. *Analyt. Cell Pathol.* 1989, 1:123-132.
7. Gilles, C., and Thompson, E.W., The epithelial to mesenchymal transition and metastatic progression in carcinoma. *Breast J.* 1996, 2:83-96.
8. Gruler, H., Directed cell movement: a biophysical analysis. *Blood Cells.* 1993, 19:91-113.
9. Hazgui, S., Bonnet, N., Cutrona, J., Nawrocki-Raby, B., Polette, M., Chouchane, L., Birembaut, P., and Zahm, J.M., 3D culture model and computer-assisted videomicroscopy to analyze migratory behavior of non-invasive and invasive bronchial epithelial cells. *Am. J. Physiol. Cell Physiol.* 2005, in press.

10. Huettner, P.C., Weinberg, D.S. and Lage, J.M., Assessment of proliferative activity in ovarian neoplasms by flow and static cytometry. *Am. J. Pathol.* 1992, 141:699-706.
11. Katsumi, A., Milanini, J., Kiosses, W.B., del Pozo, M.A., Kaunas, R., Chien, S., Hahn, K.M., and Schwartz, M.A., Effects of cell tension on the small GTPase Rac. *J. Cell Biol.* 2002, 158:153-164.
12. Marcelpoil, R. and Usson, Y., Methods for the study of cellular sociology: Voronoi diagrams and parametrization of the spatial relationships. *J. Theor. Biol.* 1992, 154:259-369.
13. Matos, M., Nawrocki Raby, B., Zahm, J.M., Polette, M., Birembaut, P. and Bonnet, N., Cell migration and proliferation are not discriminant factors in the *in vitro* sociologic behavior of bronchial epithelial cell lines. *Cel. Motil. Cytoskel.* 2002, 53:53-65.
14. Nawrocki, B., Polette, M., Van Hengel, J., Tournier, J.M., Van Roy, F. and Birembaut, P., Cytoplasmic redistribution of E-cadherin-catenin adhesion complex is associated with down-regulated tyrosine phosphorylation of E-cadherin in human bronchopulmonary carcinomas. *Am. J. Pathol.* 1998, 153:1521-1530.
15. Nawrocki Raby, B., Polette, M., Gilles, C., Clavel, C., Strumane, K., Matos, M., Zahm, J.M., Van Roy, F., Bonnet, N. and Birembaut, P., Quantitative cell dispersion analysis: new test to measure tumor cell aggressiveness. *Int. J. Cancer* 2001, 93:644-652.
16. Nawrocki Raby, B., Gilles, C., Polette, M., Martinelle-Catusse, C., Bonnet, N., Puchelle, E., Foidart, J.M., Van Roy, F. and Birembaut, P., E-cadherin mediates MMP down-regulation in highly invasive bronchial tumor cells 2003, *Am. J. Pathol.*, 163(2): 653-661.
17. Palmari, J., Andre, J.Y., Martin, P.M. and Dussert, C., Cellular automaton model of proliferation of a human breast cancer cell line. *Proc. SPIE* 1994, 2168:408-415.
18. Parzen, E., On estimation of a probability density function and mode. *Ann. Math. Statist.* 1962, 33:1065-1076.

19. Polette, M., Gilles, C., de Bentzmann, S., Gruenert, D., Tournier, J.M. and Birembaut, P., Association of fibroblastoid features with the invasive phenotype in human bronchial cancer cell lines. *Clin. Exp. Metastasis* 1998, 16:105-112.
20. Rieu, J.P., Upadhyaya, A., Glazier, J.A., Bob Ouchi, N. and Sawada, Y., Diffusion and deformations of single hydra cells in cellular aggregates. *Biophys. J.* 2000, 79: 1903-1914.
21. Sudbo, J., Bankfalvi, A., Bryne, M., Marcelpoil, R., Boysen, M., Pikkko, J., Hemmer, J., Kraft, K. and Reith, A., Prognostic value of graph theory-based tissue architecture analysis in carcinomas of the tongue. *Lab. Invest.* 2000, 80:1881-1889.
22. Ura, H., Bonfil, R.D., Reich, R., Reddel, R., Pfeifer, A., Harris, C.C. and Klein-Szanto, A.J., Expression of type IV collagenase and procollagen genes and its correlation with the tumorigenic, invasive, and metastatic abilities of oncogene-transformed human bronchial epithelial cells. *Cancer Res* 1989, 49: 4615-4621.
23. Weyn, B., Van de Wouwer, G., Kumar-Singh, S., van Daele, A., Scheunders, P., van Marck, E. and Jacob, W., Computer-assisted differential diagnosis of malignant mesothelioma based on syntactic structure analysis 1999, *Cytometry*, 35: 23-29.
24. Zahm, J.M., Kaplan, H., Herard, A.L., Doriot, F., Pierrot, D., Somelette, P. and Puchelle E. Cell migration and proliferation during the *in vitro* wound repair of the respiratory epithelium. *Cell. Motil. Cytoskeleton* 1997, 34:33-43.
25. Zahm, J.M., Raby, B., Herard, A., Puchelle, E. and Bonnet, N., Electrical field-directed cell migration during respiratory epithelium wound repair. *Proc. SPIE* 2000, 3921:190-196.

## FIGURE LEGENDS

**Figure 1:** Schematic representation of the rank attributed to cells according to their migration in the direction of high cell density, in the direction of low cell density or in a direction not related to density. A rank  $r$  was attributed to each cell ( $0 \leq r \leq 7$ ), corresponding to the

direction followed by the cell during its move from image  $t$  to image  $t + \Delta t$ . Rank 7 corresponds to a migration towards the highest cell density in the cell neighborhood and rank 0 to a migration towards the lowest cell density.

**Figure 2:** Evolution of the spatial distribution of cells from 5 different cell lines at different time intervals ( 1 hour after seeding; 9 hours after seeding; 17 hours after seeding). The non-invasive 16HBE14o- and MCF7 cells progressively formed clusters over time, whereas the BRZ and BT549 cells did not. The MCF10 cells had an intermediate behavior.

**Figure 3:** Evolution of the spatial distribution of 16HBE14o- cells in the directed migration model, in which cells are engaged in the wound repair process. Images were recorded at 1.5 hour intervals until the wound closure. A progressive decrease in the wound area was observed.

**Figure 4:** Illustration of the different spatial repartitions observed for invasive (A, B, C: BZR) and non invasive (D, E, F: 16HBE) cell lines. The left column displays the positions of cells after 17 h of culture. The middle column represents the Voronoï diagram computed from these positions and the right column represents the Delaunay triangulation. One can observe that the formation of clusters typically occurs with non invasive cells (arrows in D). This qualitative interpretation is confirmed when quantitative descriptors of the Voronoï partition (G) and the Delaunay triangulation (H) are computed. The descriptors remain constant for the BZR cells whereas a decrease of RFH and increase of AD and a decrease of M and increase of SD is observed for the 16HBE cells.

**Figure 5:** Quantification of the degree of attraction-repulsion for 16HBE14o- (A, B, C) and BZR (D, E, F) cell lines. A-B and D-E represent 2 consecutive images ( $\Delta t = 100$  min) recorded from the 16HBE14o- and BZR cells, respectively. In C and F, the direction of migration of cells is superimposed on the estimated cell density (a white coloration represents a high cell density).

**Figure 6:** Representation of the index of density-based attraction versus time for 5 cell lines and for the model of directed migration. The index of density-based attraction value is close to 0 for non-invasive cells as well as for invasive cells, indicating that a mechanism of no global-attraction/repulsion governs their migration. The index value determined from the directed migration model, close to +1, reflects a model of global attraction.

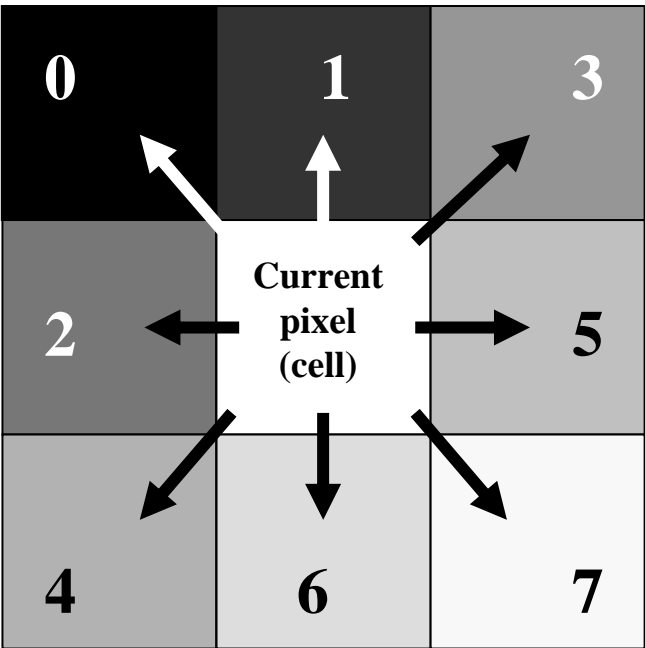


Figure 1

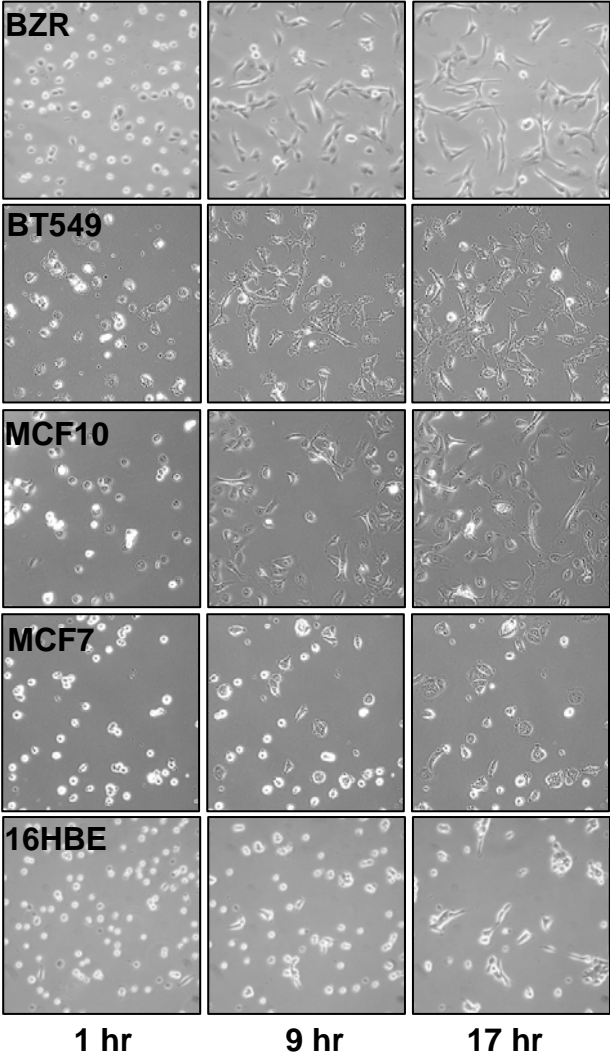


Figure 2

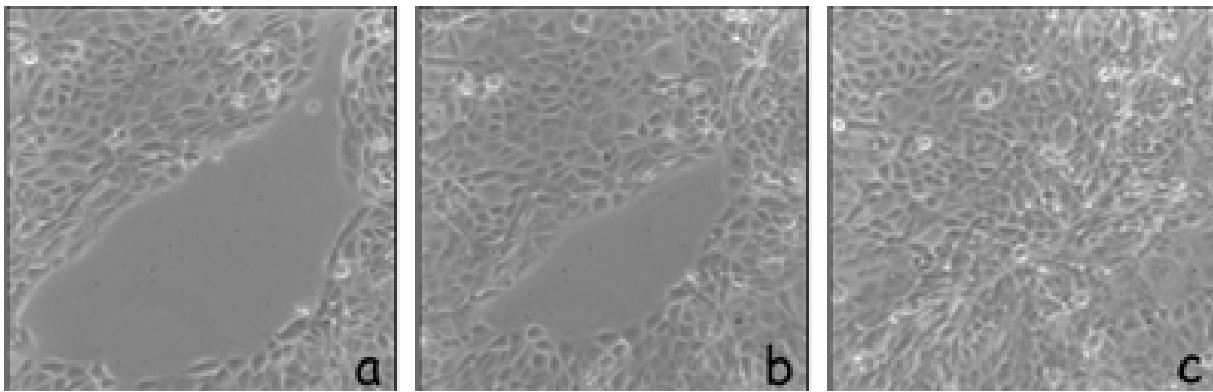


Figure 3

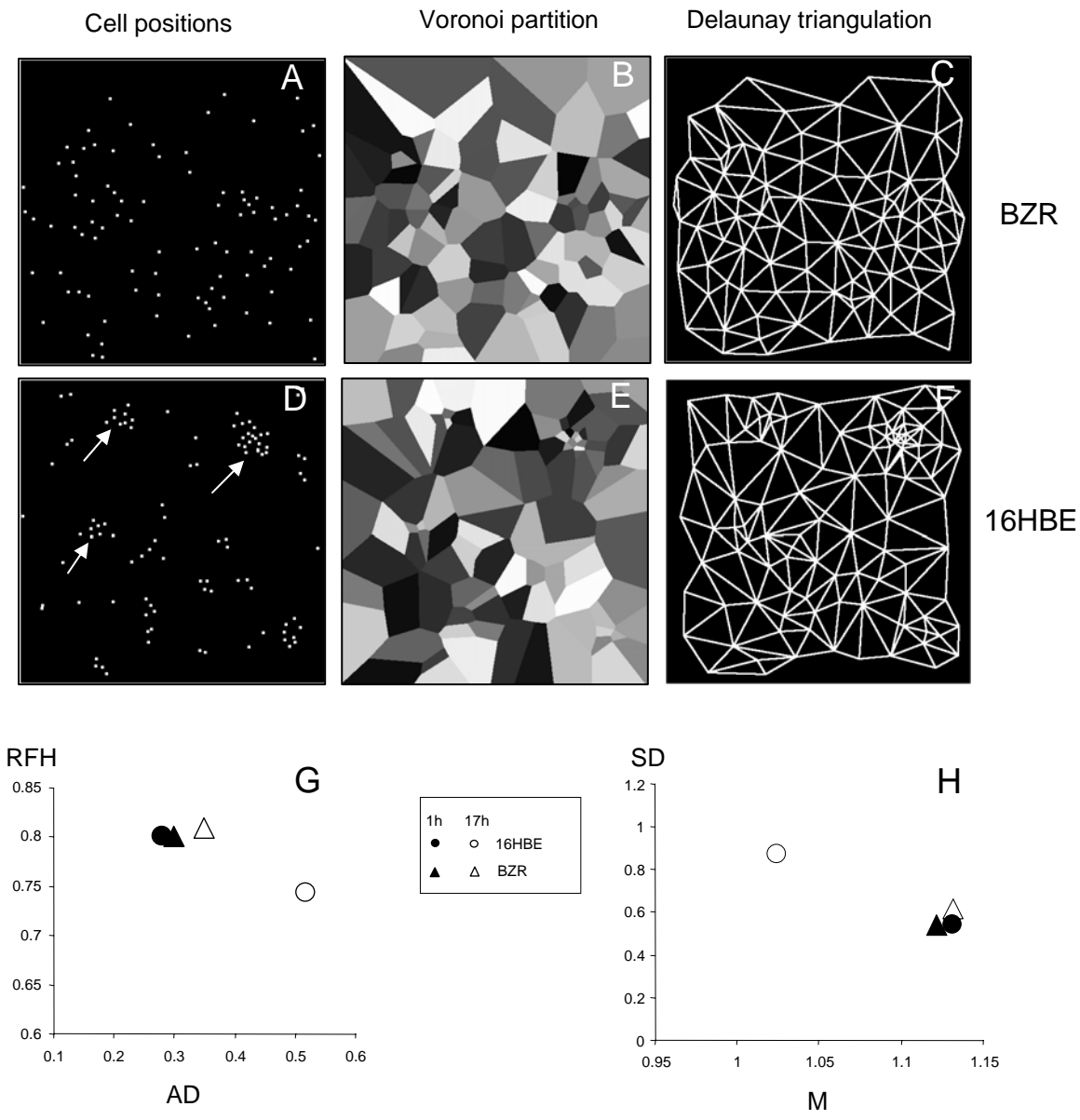


Figure 4

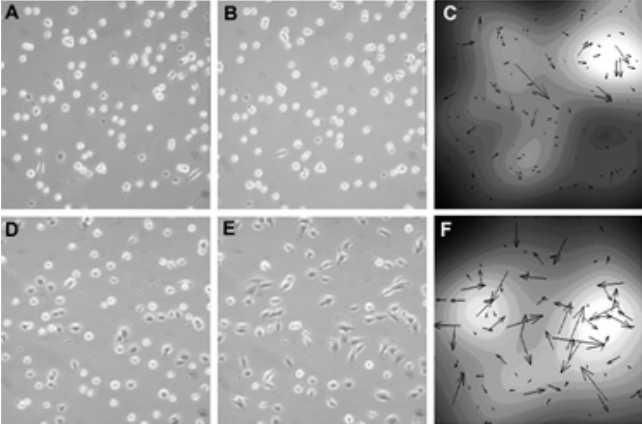


Figure 5

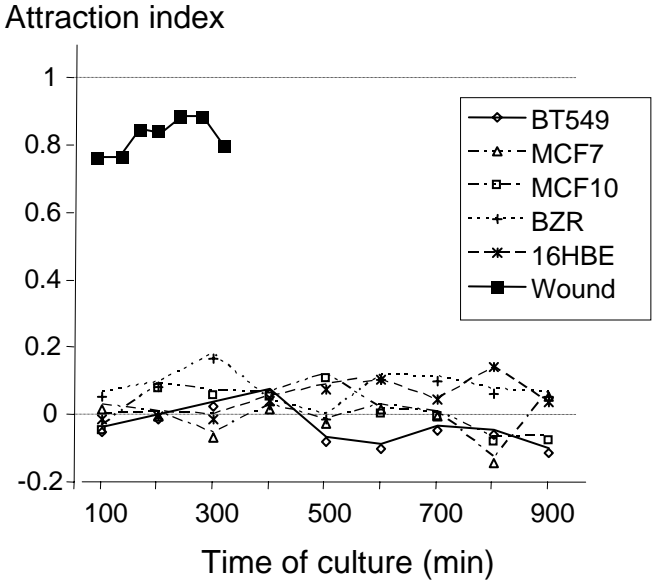


Figure 6